Sumer Journal for Pure Science (ISSN: 2790-7031)
2nd International Scientific Conference on Pure and Medical Sciences/University of Sumer 2024

Nano Silver Particles Modified with Pectin and Their Application in Biomedical

Muayad Rahim Hussein[1], Asmaa Hadi Mohammed[2], Farah T. M. Noori[3]

[1]*Physics Department/ College of Science /University of sumer / Thi-Qar/Iraq.*
[2]*Physics Department / College of Science /Al- Nahrain University/Baghdad/Iraq.*
[3]*Physics Department/College of Science /University of Baghdad/Baghdad/Iraq.*

***Corresponding author: mouidrahiem@gmail.com**

Abstract

Nanomaterials are important for the formation of silver nano particles (AgNPs), silver and pectin (Ag @Pc) complex was synthesized by two methods, namely laser ablation (PLA)and electrochemical cell. A set of tests have been conducted for this overlay such as: X-ray diffraction (X-ray) Analysis, Fourier Transform-Infrared Spectroscopy(FTIR)Analysis, Ultra-Violet visible (UV-Viz) Analysis, Transmission Electron Microscopy (TEM) Analysis, Atomic Force Microscope(AFM)Analysis, Scanning Electron Microscope (SEM)Analysis. X-ray examinations showed that the material has a polycrystalline nanostructure, with an average size of 20 nm, the highest peak intensity was at the angle of θ=38°, A spherical shape for particles was a Face Center Cubic (F.C.C) type with a dominant plane (111). However, there is little difference between the two methods with a level of crystallization. As for the FTIR examination, it was found that the ideal absorption at the beams wave numbers 1588 cm-1 and 3340 cm-1, which is identical to the elongation frequency for Assignments (-COO, -OH) as a stretching vibration, respectively for both methods. As for the UV-Vis examination, the absorption peak was at the wavelength of 437 nm. Further, for the TEM examination, the XRD examination was strengthened having the same Nano structured shapes as a spherical shape. As for the SEM images of Ag@Pc films revealed nanometer-sized objects AgNPs are globular and evenly distributed throughout the inspected region. A less regular shape of AgNPs may indicate nanoparticle agglomerates more. As for AFM the image of the AgNPs@pectin film is slightly blurred, suggesting the effect of viscosity for the biological part, the material was examined Antibacterial activity for four types of gram-negative and gram-positive bacteria, namely (Staphylococcus aureus, Salmonella tophi, Klebsiella pneumoniae and Escherichia coli (E-coli)) with inhibition zone which were approximability 23, 21, 18 and 19 mm, respectively with plasmolysis of the cell wall and separation of the cytoplasm. However, the nano products synthesized by laser method was less efficient than in the electrochemical method due to its concentration and less impurities. More, the medical part, application of the nano products on one type of cancers, which is skin cancer. The concentration of the substance ranged from 70-160 µg / mole. Silver and pectin showed toxicity to cancer cells, so it inhibited them depending on the concentration and period of application. The time in this case was from 0 to 120 min, at which the effect of silver and silver @ pectin was suppression of related protein. Skin cancer, it took the same concentration, but it was noted that concentration and time were also taken into account, but it was noted that silver with pectin stopped the migration of cancer cells by 50%, while silver 60%, Silver by 30 %. As for skin cancer, for the same concentration of 70 – 160 µg/ mole for same period, it was observed that it reduces the protein concentration. Western blot method was used to find out the protein concentration.

Keywords: Pectin, Cancer Therapy, AgNPs, AgNPs/pectin

الجسيمات النانوية المعدلة بالبكتين وتطبيقاتها في الطب الحيوي

مؤيد رحيم حسين [1]*, اسماء هادي محمد [2], فرح طارق محمد نوري [3]

[1] قسم الفيزياء – كلية العلوم جامعة سومر–, ذي قار ,العراق

[2] قسم الفيزياء – كلية العلوم جامعة النهرين , بغداد , العراق

[3] قسم الفيزياء – كلية العلوم جامعة, بغداد, بغداد, العراق

الخلاصة

تعتبر المواد النانوية مهمة لتكوين جزيئات الفضة النانوية (AgNPs)، وتم تصنيع الفضة والبكتين (Ag @Pc) بطريقتين، وهما الاستئصال بالليزر والخلية الكهروكيميائية. تم إجراء مجموعة من الاختبارات لهذا التراكب مثل: تحليل حيود الأشعة السينية(X-ray) ، تحليل فورييه للتحليل الطيفي للأشعة تحت الحمراء(FTIR) ، تحليل الأشعة فوق البنفسجية المرئية(UV-Viz) ، الفحص المجهري الإلكتروني للإرسال (.(TEM) التحليل، تحليل مجهر القوة الذرية(AFM) ، تحليل المجهر الإلكتروني الماسح .(SEM) أظهرت فحوصات الأشعة السينية أن المادة لها بنية نانوية متعددة البلورات، بمتوسط حجم 20 نانومتر، وكانت أعلى شدة ذروة عند الزاوية θ=38 –، وكان الشكل الكروي للجزيئات من النوع مكعب مركز الوجه (F.C.C) مع الطائرة المهيمنة (111). ومع ذلك، هناك اختلاف بسيط بين الطريقتين فيما يتعلق بمستوى التبلور. أما بالنسبة لفحص FTIR فقد وجد أن الامتصاص المثالي عند الحزم ذات الأرقام الموجية 1588

Sumer Journal for Pure Science (ISSN: 2790-7031)
2nd International Scientific Conference on Pure and Medical Sciences/University of Sumer 2024

سم-1 و 3340 سم-1 وهو مطابق لتردد الاستطالة للتخصيصات (-COO, -OH) كاهتزاز تمدد على التوالي. لكلا الطريقتين. أما بالنسبة لفحص الأشعة فوق البنفسجية والمرئية، فقد كانت ذروة الامتصاص عند الطول الموجي 437 نانومتر. علاوة على ذلك، بالنسبة لفحص TEM، تم تعزيز فحص XRD بحيث يحتوي على نفس الأشكال النانوية المهيكلة كشكل كروي. أما بالنسبة لصور SEM لأفلامAg@Pc ، فقد كشفت عن كائنات بحجم نانومتر AgNPs كروية وموزعة بالتساوي في جميع أنحاء المنطقة التي تم فحصها. قد يشير الشكل الأقل انتظامًا لـ AgNPs إلى وجود تكتلات جسيمات متناهية الصغر أكثر. أما بالنسبة لـ AFM فإن صورة فيلم AgNPs@pectin غير واضحة قليلاً، مما يوحي بتأثير اللزوجة للجزء البيولوجي، تم فحص المادة النشاط المضاد للبكتيريا لأربعة أنواع من البكتيريا سالبة الجرام وإيجابية الجرام وهي (المكورات العنقودية الذهبية، السالمونيلاTophi ، Klebsiella pneumoniae وE-coli)) Escherichia coli (مع منطقة تثبيط كانت تقريبية 23، 21، 18 و 19 ملم، على التوالي مع تحلل جدار الخلية وانفصال السيتوبلازم. إلا أن منتجات النانو المصنعة بطريقة الليزر كانت أقل كفاءة منها بالطريقة الكهروكيميائية بسبب تركيزها وقلة الشوائب. المزيد، الجزء الطبي، تطبيق منتجات النانو على نوع واحد من السرطانات وهو سرطان الجلد. تراوح تركيز المادة بين 70-160 ميكروغرام/مول. أظهرت الفضة والبكتين سمية للخلايا السرطانية، فتثبطها حسب التركيز ومدة التطبيق. كان الوقت في هذه الحالة من 0 إلى 120 دقيقة، حيث كان تأثير الفضة والبكتين الفضي هو قمع البروتين ذي الصلة. سرطان الجلد، أخذ نفس التركيز، ولكن لوحظ أنه تم مراعاة التركيز والوقت أيضًا، ولكن لوحظ أن الفضة مع البكتين أوقفت هجرة الخلايا السرطانية بنسبة 50%، بينما الفضة 60%، والفضة بنسبة 30%. . أما بالنسبة \السرطان الجلد فعند نفس التركيز 70 – 160 ميكروجرام/ مول لنفس الفترة لوحظ أنه يقلل من تركيز البروتين. تم استخدام طريقة اللطخة الغربية لمعرفة تركيز البروتين.

1. Introduction

Nanotechnology is science, engineering, and technology at the nanoscale. It is the understanding, manipulating and controlling of matter nevertheless, 100 nm as an upper limit for a nanomaterial is not always accepted .Many organizations in the world fixed different thresholds for the table [1]. It is the study and application of extremely small things. The expression "nanotechnology" is being used across all other science fields, such as chemistry, biology, physics, materials science, and engineering [2].Nano is an "extremely small" prefix. It is driven from the Greek word "Nanos" which means "dwarf". At the size-scale between individual atoms and bulk materials, where unique phenomena allow for novel uses [3]. A nanometer is one-billionth of a meter, or about the width of 10 side-by side arranged hydrogen atoms in a line. Nanotechnology involves the imaging, measurement, modeling and manipulation of material at this size [4]. Nanoparticles' smaller size and ratio of surface area to volume are the key features that makes them beneficial in biomedical fields due to the development of so many new properties, ease of functionalization, bimolecular conjugation etc.[5]. Nanoparticles can serve as an excellent bridge between molecular or atomic structures and bulk materials. The advent of nanoparticles along with other nanomaterials has opened up new avenues in many different fields of research and study[6]. Equally influenced has also been the field of biomedical engineering. The main advantages of nanoparticles over larger particles are their high surface-to - volume ratio and therefore higher surface energy, different optical, electronic, and outstanding magnetic properties, etc.[7].

In general, using bio/plant extracts to make metal nanoparticles is preferable to using microbes since it is simpler to scale up, poses less biohazard, and can shorten the time-consuming process of sustaining cell culture. An anionic polymer called pectin is extensively used in the current studies. It is a naturally occurring polymer with carboxylic groups fictionalized (fig 1). It is a common element of both land plants and green algae's cell walls[8]. This polymer's primary benefit is that it gives the cell walls mechanical strength. Additionally, it is crucial for several cellular activities, including water binding, morphological development, and fruit ripening[9]. Pectin has been employed in the pharmaceutical and medical fields for a variety of purposes, including as a detoxicant, a way to regulate cholesterol levels, an anticancer agent, a chemosensitizer, a component of controlled-release dosage forms, and a drug delivery vehicle [10][11][12][13]

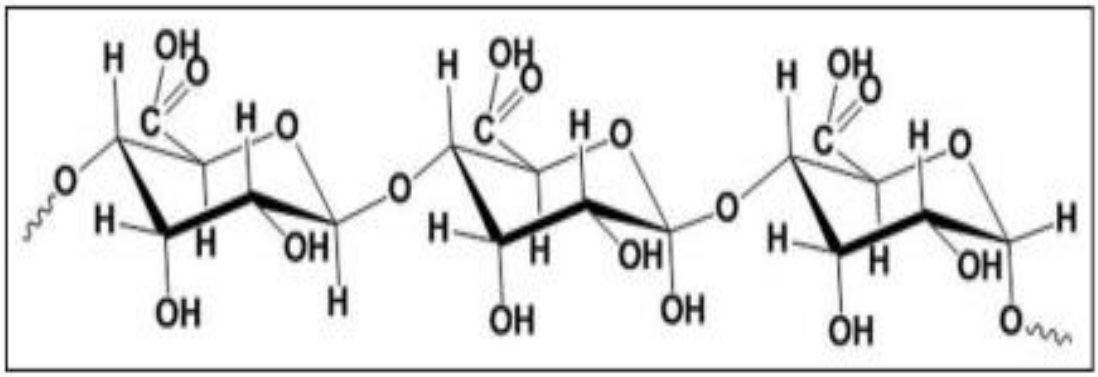

Figure -1 Chemical structure of pectin is depicted schematically

2. Material and Method

2.1 Silver and pectin by Puls laser ablation method

We use the puls laser ablation to create pectin NPs, Ag NPs, and Ag:pectin NPs in deionized water in order to compare their Electrochemical characteristics to those of Ag and pectin NPs under the same experimental conditions. Single particles and nanostructures are created using one- and two-step processes, respectively. It should be observed that the procedure an d timing of particle creation differ noticeably between those of Ag and pectin NPs. In Fig. (2a), the experimental setup is depicted. An Nd:YAG laser operating at a wavelength of 1064 nm with a pulse duration of 8 ns, a repetition rate of 2 Hz, and an energy of 420 mJ/pulse abraded the metal plate (>99.99 percent) after being put on the bottom of a glass jar with 1.5 ml of deionized water A 100 mm convergent lens was employed to concentrate the laser beam onto the metal plate. The two-step procedure used to create the Ag: pectin structures is depicted in Fig.(2b).First, a glass jar with a 2-mm-thick silver plate on the bottom was positioned 10 mm from the solution surface in the solution. For 60 minutes, the silver plate was constantly ablated. Second, a pectin plate of equal size was ablated for 60 minutes using the same laser and laser pulse energy in the first step's generated Ag colloid. To create the (Ag: pectin NPs, Ag NPs, and pectin NPs) for comparison, a sliver (or pectin) plate was ablated for 60 minutes in deionized water using the same laser at the same Characterization XRD, FTIR

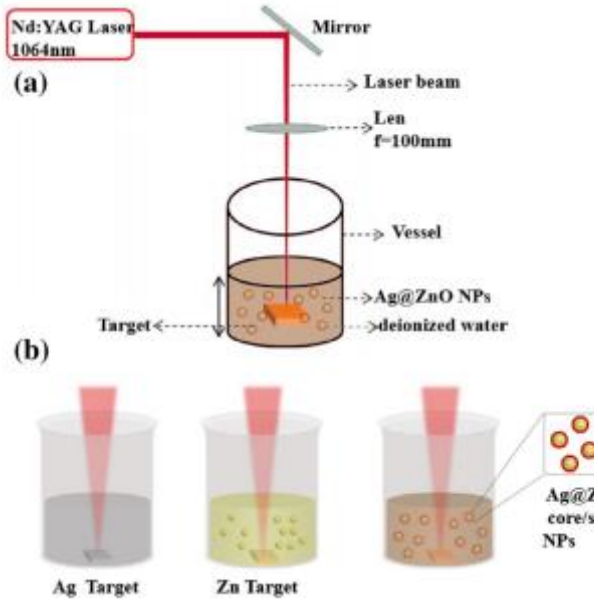

Figure -2 (a)schematic representation of the PLALsetup(**b)** The Ag: pectin nanostructures' synthesis technique

2.2 Silver and pectin preparation by chemical method

The method of preparing (Ag: Pectin) nanoparticles was done at Pectin powder and absolute ethanol were used for producing (Ag:Pectin) nanoparticles by adding drop wise AgNO3:Pectin in ethanol with 1:10 ratio under centrifuge for around 8 hours. The reaction was performed at room temperature ~23 °C. The solution was left to rest and cool back at room temperature for 2 hours, then after that measured the pH of the solution in the range of (3-15).

2-2-1 Silver and pectin preparation by electrochemical method

Electrochemical anodization was carried out in a two-electrode cell using power source (PS-3030), where the Ag foil was used as the anode and cathode electrode in this work. Anodization electrolytes were fabricated by using above solution (Pectin:Ag) with 32 volts. Each potential static anodization was performed under the room temperature of ~23 °C, after a certain period of anodization for 2 hours, The final solution was dried at 80˚C until became powder, the experimental setup shows in figure (2).

3. Antimicrobial activity of Ag and Ag: pectin Nanoparticles

By using the well diffusion method, the antibacterial activity of silver nanoparticles (Ag NPs) and silver: pectin, which were produced using various methods, was evaluated against harmful organisms such(Staphylococcus aureus, Salmonella typhi, Klebsiella pneumoniae, and Escherichia coli). Pure organism cultures were subcultured on Muller-Hinton broth at 35°C and 200 rpm using a rotary shaker. On Muller-Hinton agar plates, 6 mm-diameter wells have been created using gel puncture. On the different plates, each strain was uniformly swabbed with a sterile cotton swab. 20 l (0.002 mg) of the sample nanoparticle solution was pipetted into each plate's well using a micropipette. The various degrees of zone of inhibition were assessed following an 18-hour incubation period at 35°C.

4. Results and Discussions

4-1-1 X-Ray diffraction of pectin and silver by laser method

The diffractogram of Pectin showed a widening peak at 2θ = 20°figur(3)(a). The analysis showed that there is a decrease in the degree of crystallinity (see figure (4-1) (c). The XRD peaks of the silver nanoparticle are depicted in Figure (3) (b). The observed peaks correspond to the following Ag values: (111), (200), (142), (220), and (311) with angls(32,45,57,59,69,78). The crystallites are mostly oriented in this plane, as seen by the high intensity at θ=38° reflection. According to Dorobantu et al.,[14][15] temperatures below 30°C are primarily to blame for the creation of Ag from AgO. The broader reflections showed that AgNP crystals are smaller in size. Using the Scherer formula found in equation(1), the size of crystals D was calculated . Where is the full width at half maximum (FWHM) in radians, is the angle of reflection, and the wave length of the X-ray was employed. The average AgNPs crystallite size was found to be 20 nm. The largest peak, at 2 = 38°, corresponds to spherical nanoparticles that crystallized in the FCC structure with the (111) lattice.

$$D = k\,\lambda/\beta \cos\theta \text{ nm} \qquad [16]$$

Where D is the crystalline size(nm), λ(1.5418) is the wavelength of X-ray(nm), θ is Bragg diffraction angle, β is the full-width at half maximum (FWHM) of diffraction peak(radian) and K is Scherer's constant (0.9). The X-Ray of silver contains six peaks (see figure (3)(b) agree with [17][16], and the pectin contains only one peak. When mixing them, we notice that the number of peaks after mixing has become only three peaks. We can say that adding the pectin to the silver works to give the silver a more order, as the material contains only three peaks.

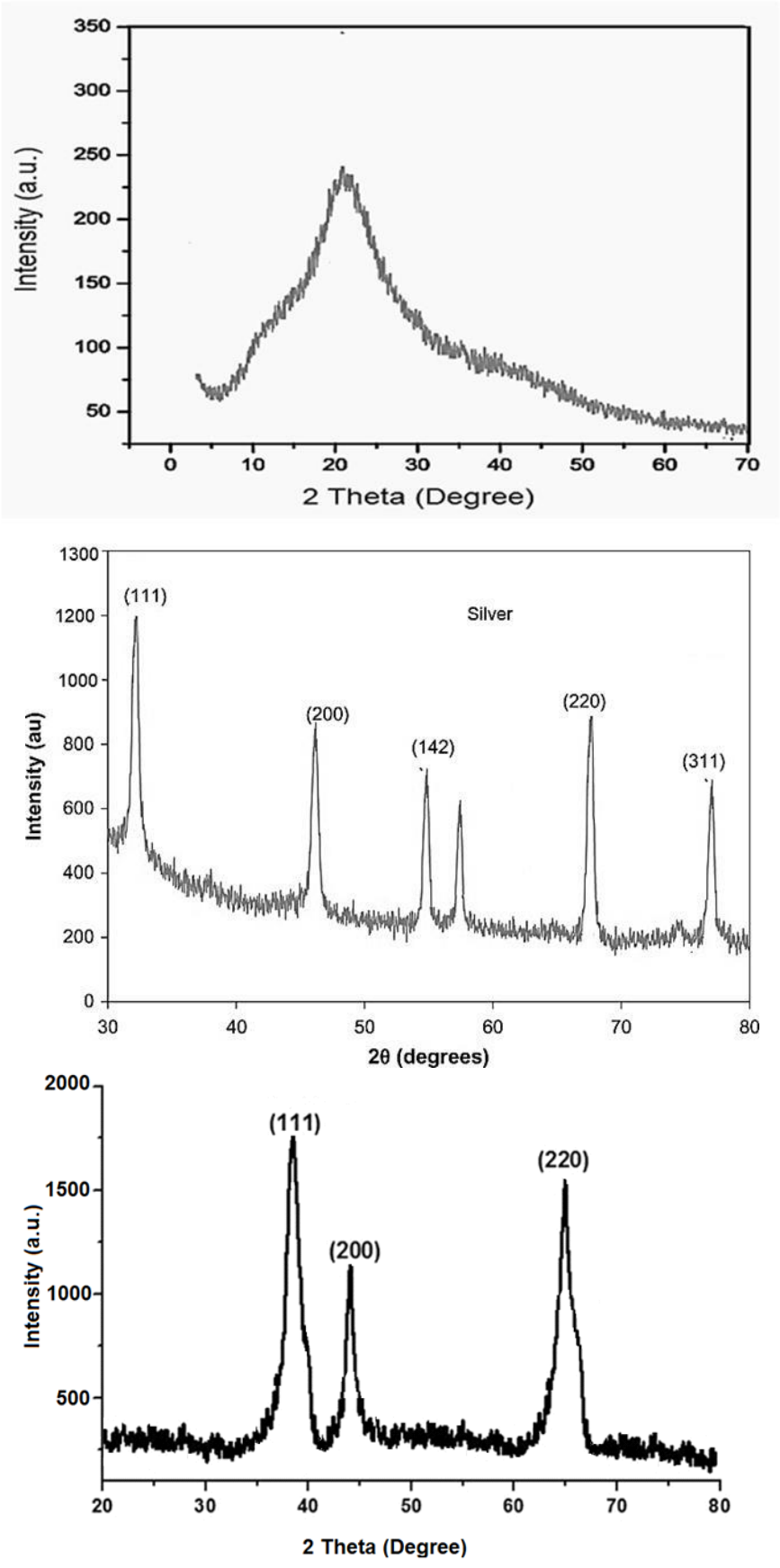

Figure -3 XRD pattern of (a)) pectin, (b) AgNPs and (c) AgNPs@pectin by using laser method

4.1-2 X-Ray Diffraction Analysis for Nano products Synthesized by Electrochemical Method

Figure (4) represents the XRD pattern of Ag:pectin nanostructure. It is found that three sets of diffraction peaks, including XRD peaks of Ag:pectin, correspond to the face-centred structure of Ag (JCPDS card no. 04-0783). Compared to the diffraction peaks in Ag NPs and Ag: pectin NPs, no noticeable shift in the diffraction peaks of Ag and pectin in Ag:pectin NPs is observed, absence of other impurity diffraction peaks suggests high purity of the Ag:pectin nanostructure synthesized by electrochemical method.A comparison have been made between the silver that was prepared by the laser atomization method mixed with pectin, and the silver that was prepared by the electrolytic cell method, see figure (4) which was mixed with pectin. The difference noticed was:

1- A change in one of the levels in the chemical and it is changed to (220) in the laser.
2- There was a displacement at the main peak.
3- That was because of the disappearancey of impurity.

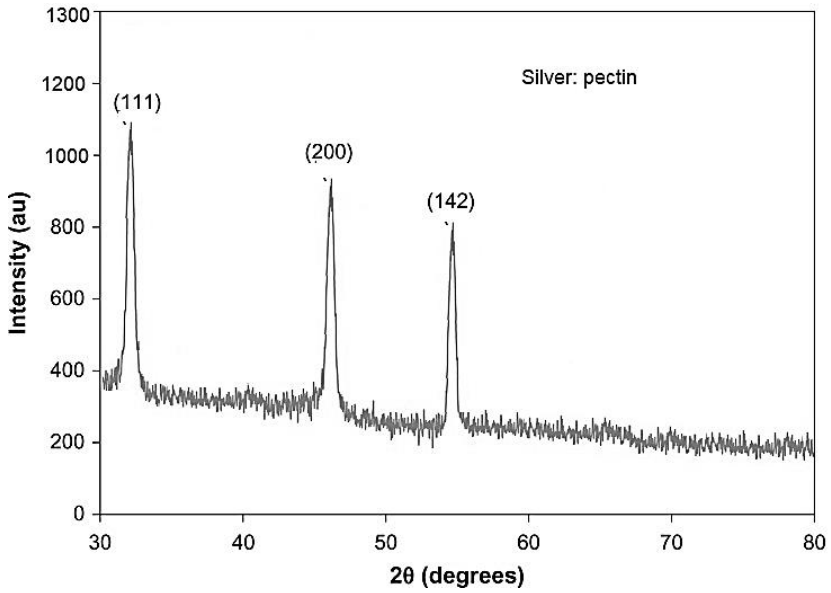

Figure -4 XRD pattern of (a) pectine (b) AgNPs and (b) AgNPs/pectin by using electrochemical method.

4.2 FTIR spectra of AgNPs/pectin prepared by using laser method

One of the greatest methods for spotting a silver-macromolecule interaction is FTIR spectroscopy. The typical absorption band at 1630 cm-1 and 3442 cm-1 corresponds to the stretching frequency of the -COO and -OH groups, respectively. Figure (5) displays the FTIR spectra of P-Ag and the FTIR spectra of pure pectin. The -C-H stretching vibration is what causes the band to be at 2920 cm-1[30]. The bands at approximately 1416 and 1386 cm-1 are attributed to, respectively, -CH2 scissoring and -OH bending vibration. The band at 1116 cm-1 is caused by the stretching of [-CH-O-CH2]. However, the FTIR spectra of P-Ag show comparable characteristic bands with just tiny variations in their vibrational frequencies (1630 [-COO], 3442 [-OH], 2841 [-CH2], and 9867[-CH-O-CH2]). A substantial connection between SNPs in P-Ag and the chains of the pectin polymer is suggested by the data, which conclude

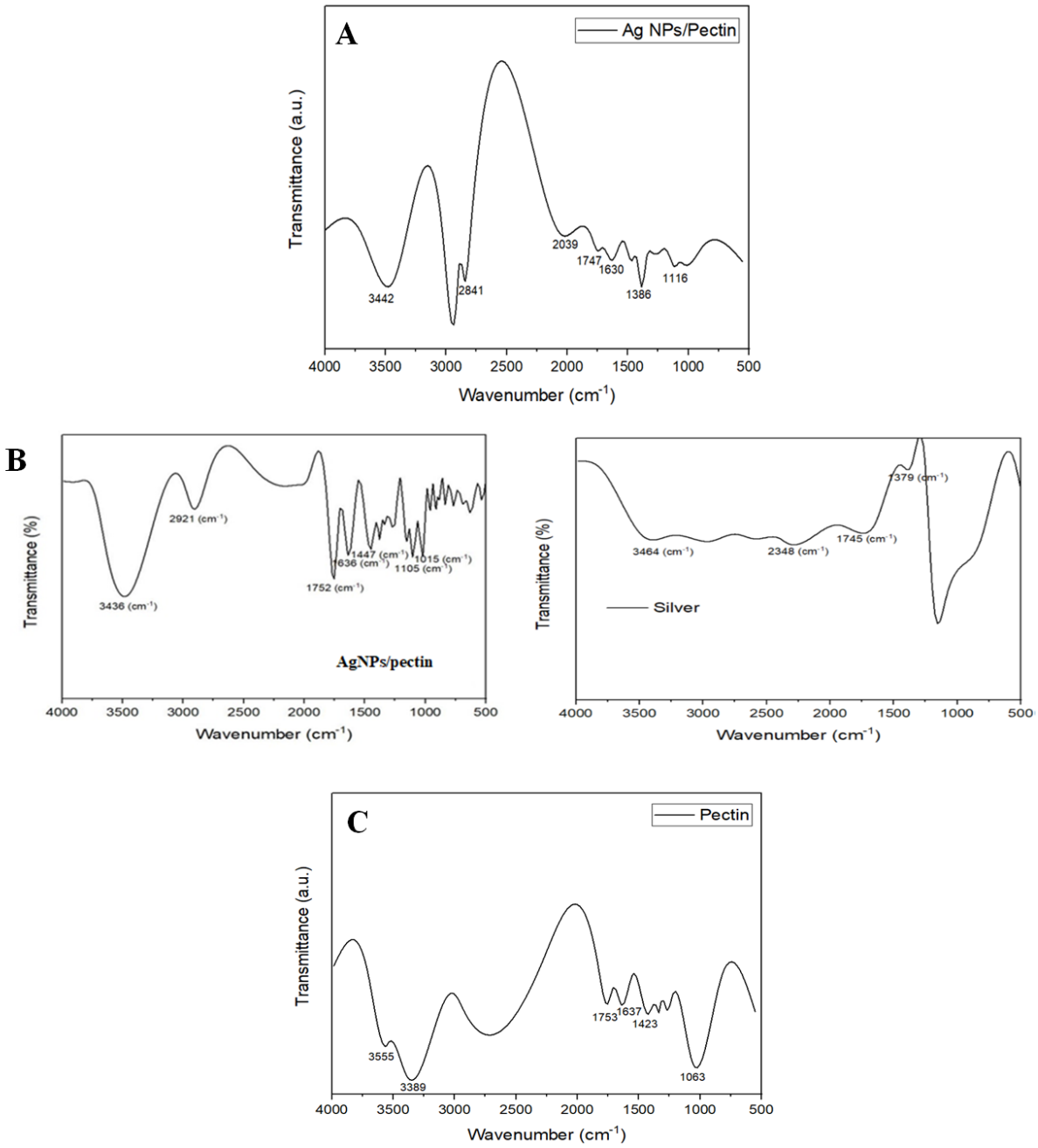

Figure -5A FTIR spectra of AgNPs/pectin prepared by using laser method, B, FTIR spectra of AgNPs/pectin prepared by using electrochemical and C represents FTIR spectra of pectin.and silver.

Table 1- Bonds for FTIR by laser

Wave number (cm)	Vibration type	Assignment
3442	stretch	- OH
2841	stretch	-CH2
2290	Strech	C-H
1386	Bending	OH
1416	scissoring	-CH2
1116	stretch	-CH-O-CH2
1015	Wagging	C-H
1630	Stretch	-COOH

Table 2- Bonds for FTIR by electrochemical

Wave number (cm)	Vibration type	Assignment
1447	Stretch	-COO
3436	Stretch	-OH
2291	Stretch	-C-H
1416	Scissoring	-CH2
1322	Bending	-OH
1019	Stretch	-CH-O-CH2

4.3 TEM analysis

4.3.1 TEM for Nano product synthesized by laser method and electrochemical method

Nanometer-sized particles were seen in the TEM images of the NMNPs/pectin films Figures(6 and 7). The area under inspection is covered with spherical AgNPs that are uniformly spaced out. AgNPs with a less symmetrical shape can be agglomerates of nanoparticles. The cracks visible in the TEM images (Figure 4) are caused by the disintegration of the carbon support film on the copper network due to the dehydration under low pressure-induced shrinkage of the pectin that was deposited. Because the pectin coating is transparent to the electron beam, it cannot be seen.[17][18]

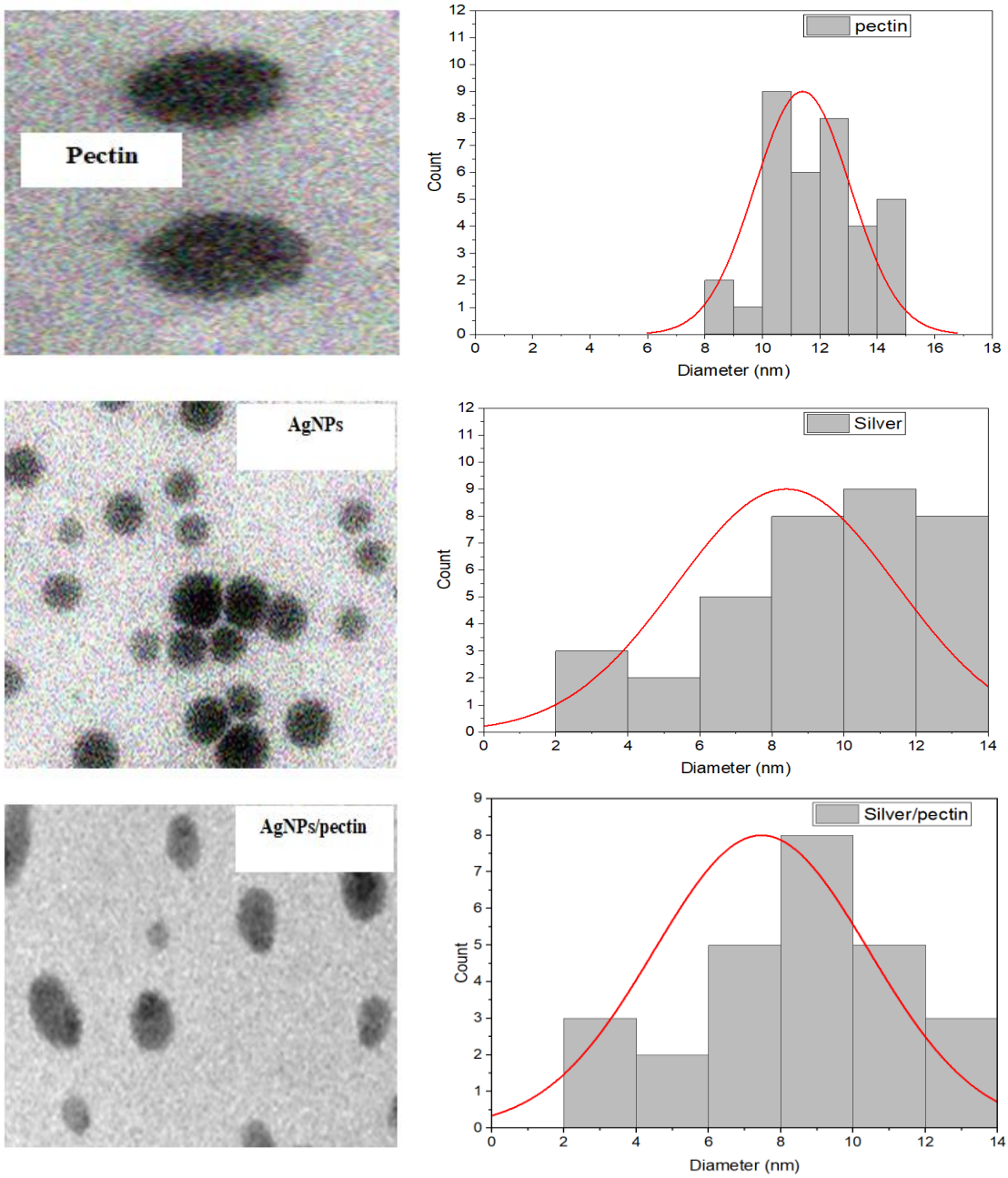

Figure -6 TEM images of (a) AgNPs and (b) AgNPs/pectin prepared by using laser ablation method

The potential approaches for examining the surface shape and size of metal nanoparticles are TEM and DLS (Figures 4). The production of SNPs in the pectin films has been amply demonstrated by the TEM image of P-Ag. The metallic silver should match the dark center of the nanoparticles. According to the TEM picture, SNPs are between 23 and 30 nm in diameter. DLS data show that the average diameter of DLS histograms is 13.5 nm.

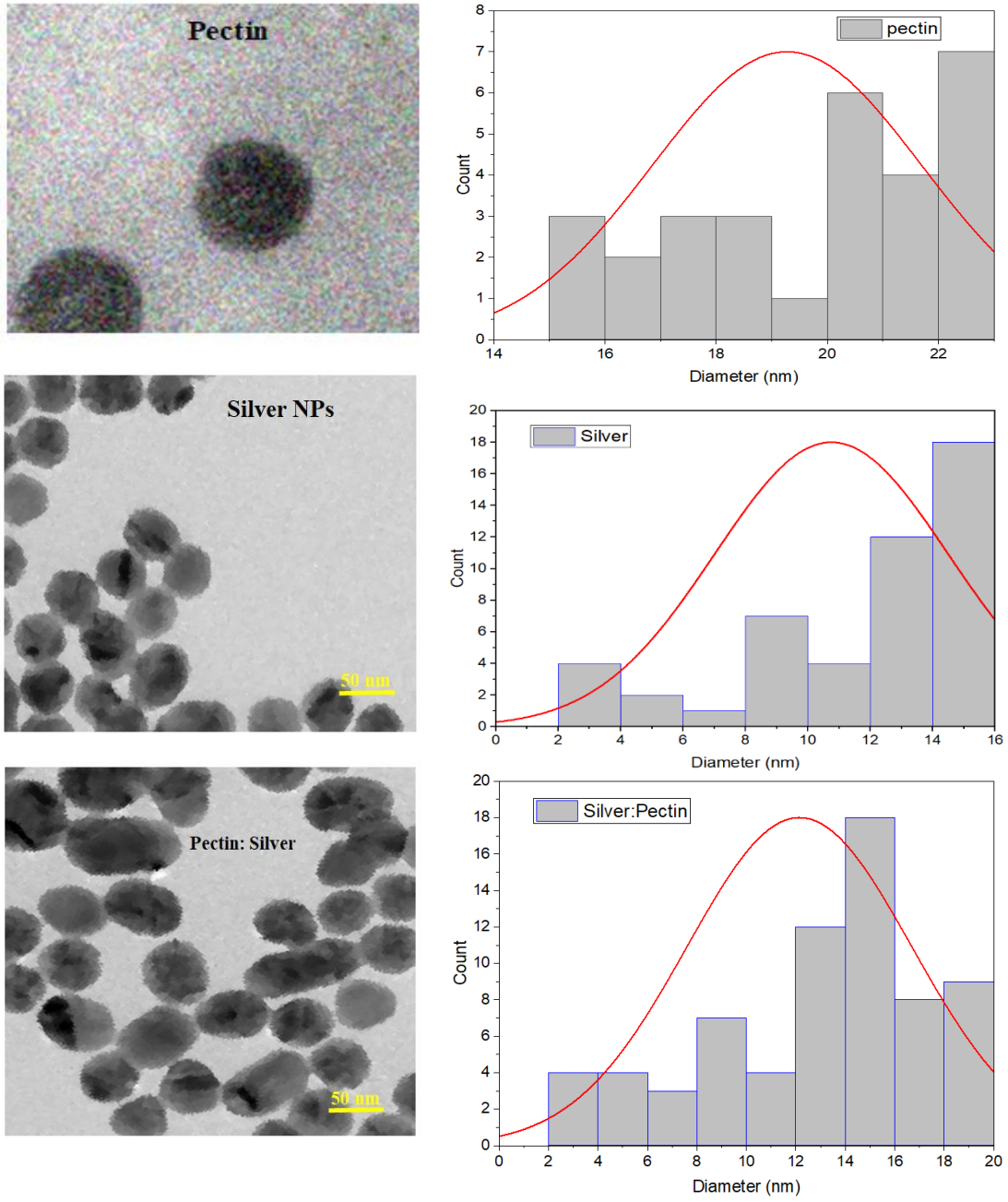

Figure -7 TEM images of (a) AgNPs and (b) AgNPs/pectin prepared by using chemical method

4.4 Atomic Force Microscoping (AFM) Anylysis

The shape and size of the silver and silver:pectin nanoparticles made using various techniques were revealed by the AFM results. Figure 8 depicts the topographical image of irregular silver and silver: pectin nanoparticles; apart from the obvious creation of nanoislands, the agglomeration of silver is clearly visible. The Ag and Ag: pectin NPs measured 40.3 and 33.8 nm in size, respectively.

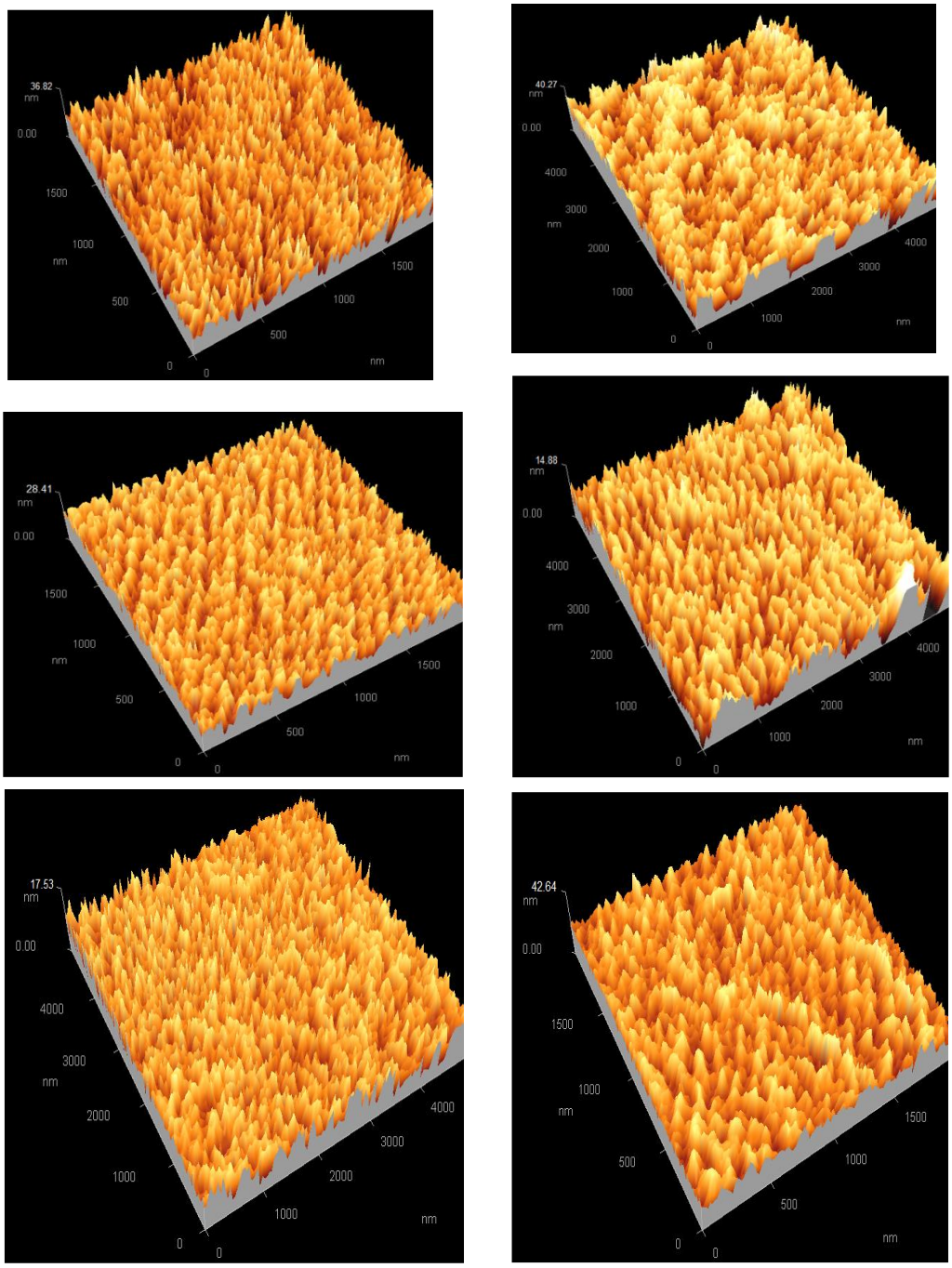

Figure -8 AFM images of (a) AgNPs and (b) AgNPs/pectin prepared by using different method

5. Application in skin cancer

Ag: Pectin NPs and their potential for penetration and accumulation into skin cancer cells were assessed to have harmful effects on cells. In order to identify variations in cellular Ag NPs and Ag, the fluorescence intensity rate as a function of incubation duration and concentration was also evaluated: Pectin NPs uptake for skin cancer cell line uptake experiments. The variation of the incubation time was 0-120 min, the Ag NPs and Ag:Pectin NPs suspended in media with two concentrations of 10 mM

and 20 mM, in addition, to control undosed cells were demonstrated as well as in figure (9) a and b respectively. Figure (9b) illustrates that Ag NPs and Ag: Pectin NPs uptake is strongly time-dependent and relatively rapid. There is a significant uptake within the first five hours for both Ag NPs and Ag: Pectin NPs. Thus, after five hours, the rate of skin cancer cells ingesting Ag NPs and Ag: Pectin NPs was markedly reduced, reaching stable values at ten hours, indicating that the cell is saturated.

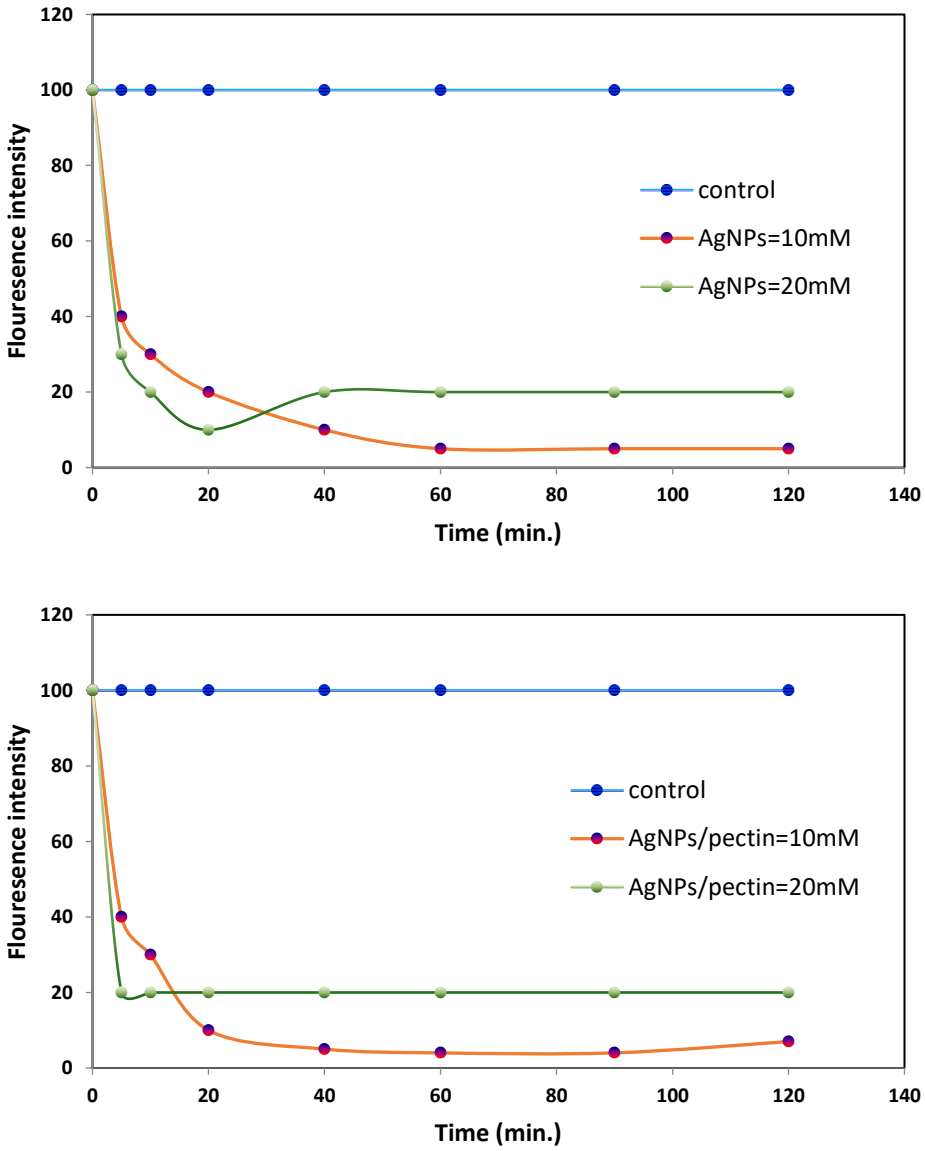

Figure -9A Fluorescence intensity rate as a function of incubation time and concentration of Ag NPs and Ag: Pectin NPs prepared by using laser method

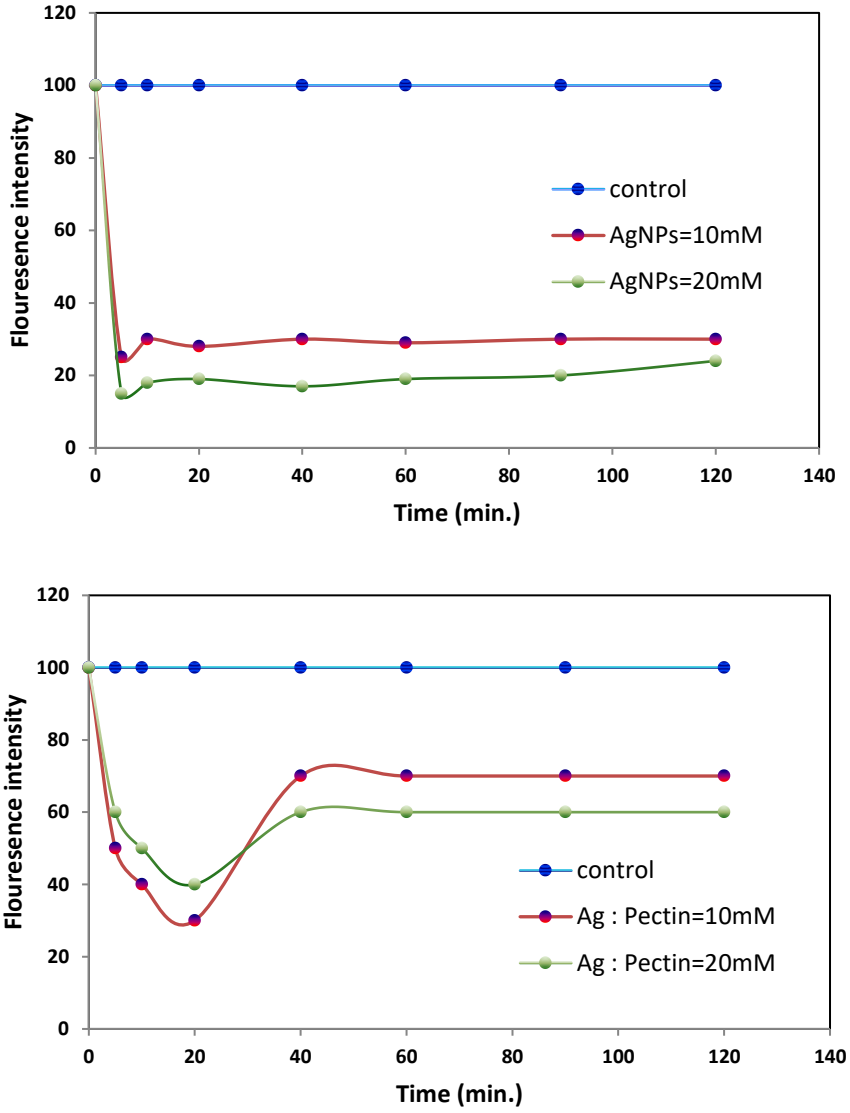

Figure -9B Fluorescence intensity rate as a function of incubation time and concentration of Ag NPs and Ag: Pectin NPs by using electrochemical method

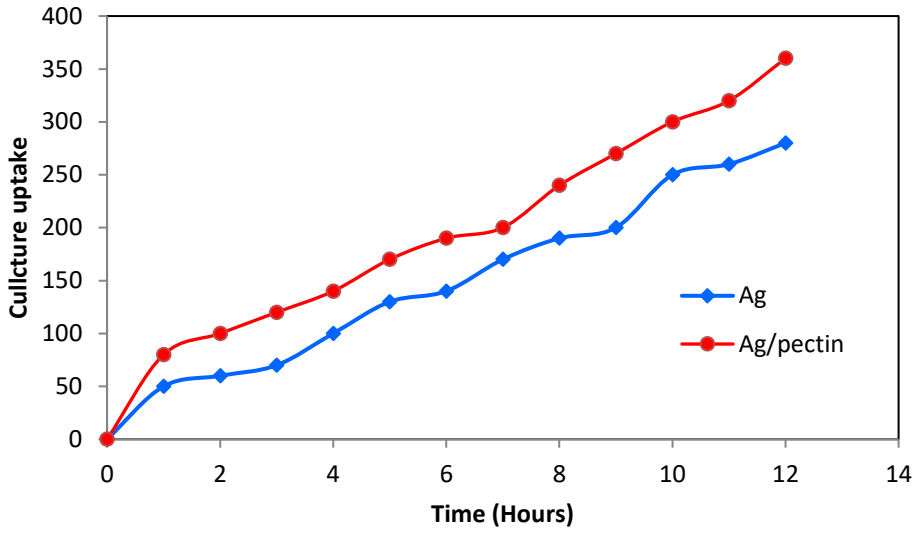

Figure 10 A- Cellular uptake of Ag NPs and Ag: Pectin NPs by using laser method

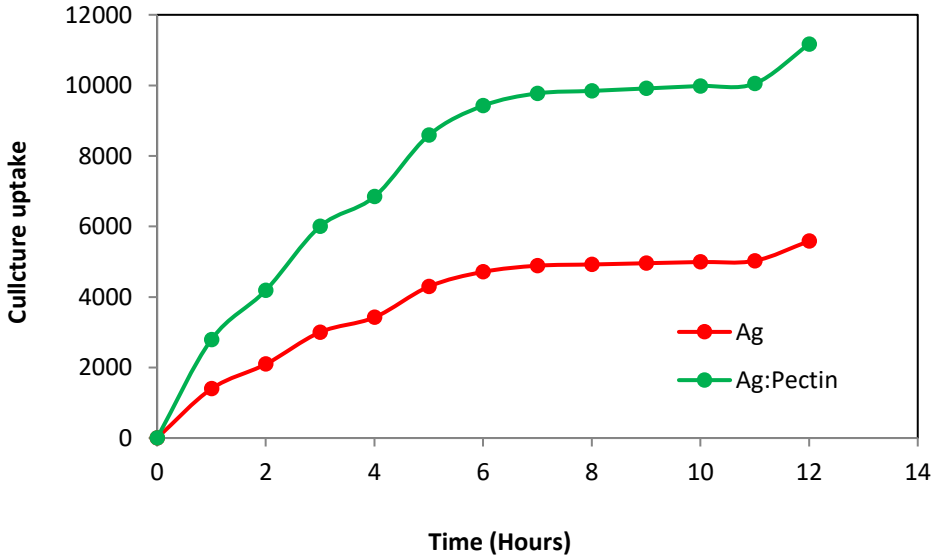

Figure -10B Cellular uptake of Ag NPs and Ag: Pectin NPs

Western blot analysis was used to see if Ag NPs and Ag: Pectin NPs affect cell migration and invasion in skincancer cells. After 24 hours of treatment with Ag NPs and Ag: Pectin NPs, Figure (8) depicts the expression levels of migration- and invasion-related proteins and their corresponding quantitative levels compared to the control group (undosed cells). As shown in the figure (8), the relative protein expression in different groups (fold) was lowered after Ag NPs and Ag: Pectin NPs treatment. Notably, Ag: Pectin NPs treatment resulted in lower protein levels than Ag NPs therapy. Ag: Pectin NPs are more effective than Ag NPs at inhibiting migration and invasion in skin cancer cells. The reason may be to the adhesion of Ag: Pectin NPs on cell membrane is more than the penetration of it as conformed in cellular uptake results, which mean that ability of Ag: Pectin NPs to interacted with membrane proteins more than the Ag NPs did. Figure (11) displays the results of western blot analysis of Ag NPs and Ag: Pectin NPs effects on cell migration and invasion. Ag NPs therapy reduced skin cancer cells' migration

ability by 60% and Ag: Pectin NPs by 50% when compared to the control group. In addition, the invasive cell rate in skin cell lines was reduced by 30% for Ag NPs and 20% for Ag: Pectin NPs treatment in skin cancer cell lines.

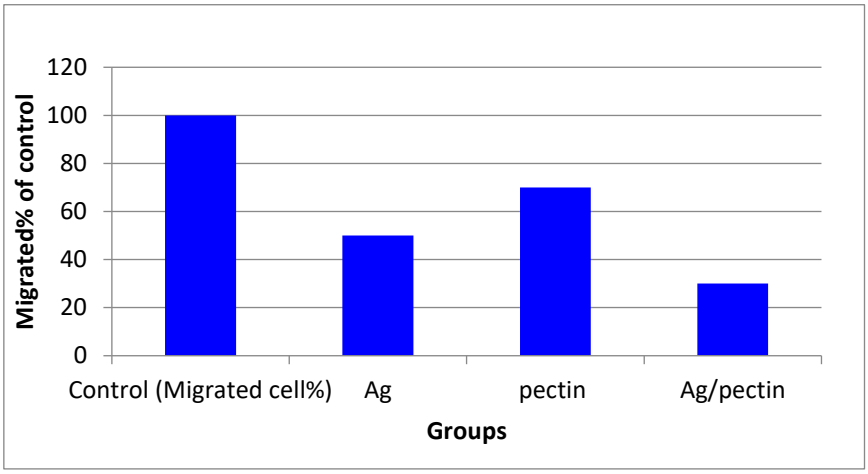

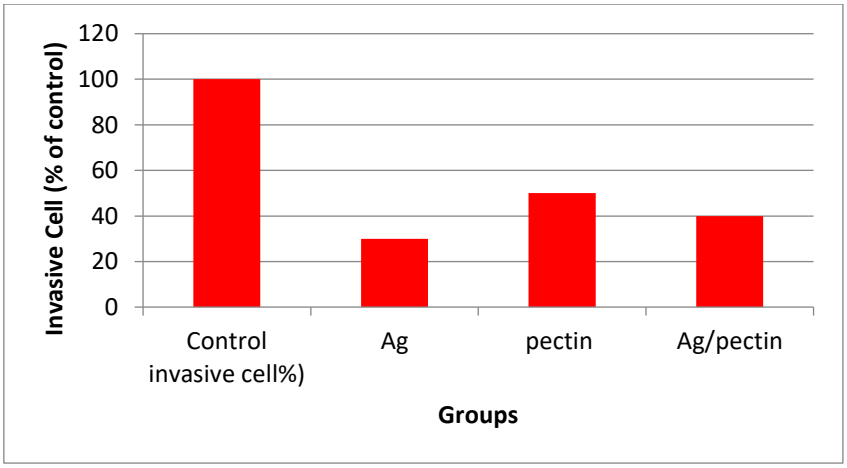

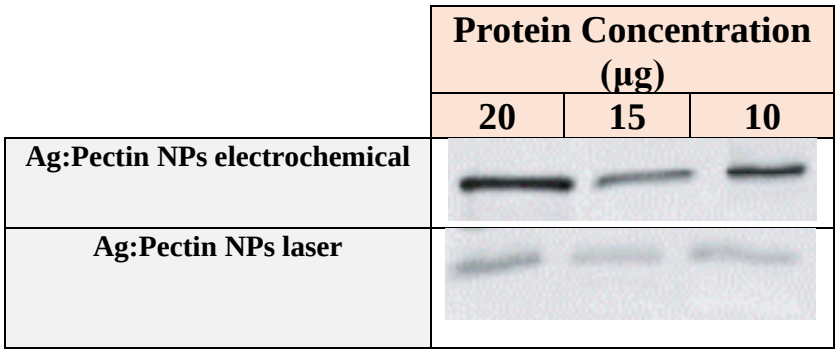

Figure -11A Migration, invasion and Western blot analysis of Ag NPs and Ag: Pectin NPs by using laser method

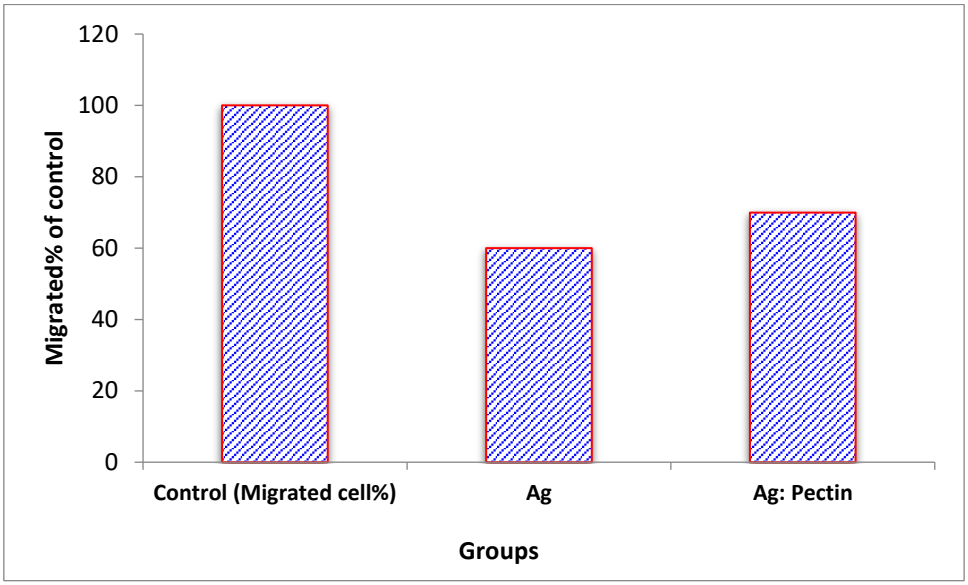

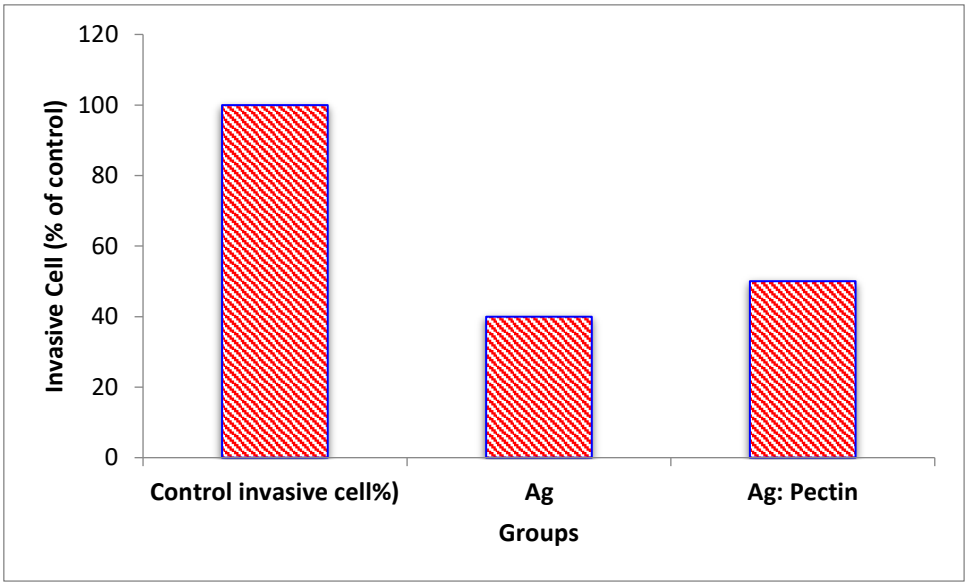

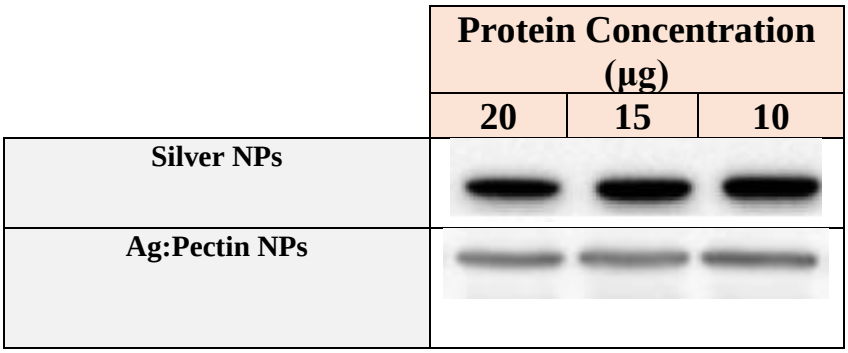

Figure -11B Migration, invasion and Western blot analysis of Ag NPs and Ag: Pectin NPs by using electrochemical method

By assessing their cytotoxicity, it is feasible to determine if created Ag NPs and Ag: Pectin NPs may have an impact on the development of skin cancer cells. In order to evaluate the cytotoxicity of human cancer cell lines, standard cell lines ($1x10^5$ ml^{-1}) were treated with increasing concentrations of Ag NPs and Ag in wells using the MTT test. Cell viability after 24 hours of exposure to pectin NPs NPs was expressed as a proportion of the untreated control (100 percent cell viability). Figures (12) and (13), respectively, display the results of cell viability after treatment with different concentrations of each Ag NP and Ag: Pectin NP (6.25, 12.5, 25, 50, 100, 200, and 400 g/ml). The cell viability curve was also used to compute the IC50 values. According to the data in figure (12), AgNPs significantly reduced skin cancer cell survival rates in a dose-dependent manner (P 0.0001) and considerably suppressed the proliferation of skin cancer cells. The data revealed that there was no difference in the cell viability rate between the control and AgNPs groups for skin cancer cells at low concentrations of 6.25 and 12.5 g/ml. Despite considerable cell absorption, Ag:Pectin NPs showed relatively negligible toxicity at doses lower than 25 g/ml. The AgNPs groups caused a significant (p 0.05) decrease in skin cancer cell survival compared to the control group at concentrations of 25 g/ml and higher, with an increase in cell killing rate occurring in a progressive order of 25 g/ml, 50 g/ml, 100 g/ml, and 200 g/ml, whereas normal cells had a regular viability rate at concentrations of 6.25 g/ml to 50 g/ml. Contrarily, it was discovered that the cytotoxic activity (IC50) against normal cells was 60 g/ml and 100 g/ml. When utilized at a higher dosage of 300 g/ml, AgNPs showed a greater mortality rate of 50% for skin cancer cells and 20% for normal cells. Ag:Pectin NPs' cytotoxicity results are illustrated in Figure (10), which demonstrates that they had a dose-dependent cytotoxic effect on skin cancer cell lines. The cell viability rate of skin cancer cells was significantly reduced by the Ag:Pectin NPs solution. The cytotoxic effects of Ag:Pectin NPs were less pronounced than those of AgNPs at specific dosesThere were no discernible changes between the control and Ag:Pectin NPs groups for concentrations ranging from 6.25 to 50 g/ml for either normal or skin cancer cell types. Despite having a strong absorption into the cells, indicates that the significant toxicity of Ag:Pectin NPs was at concentrations higher than 50 g/ml. Skin cancer cells significantly lost viability at concentrations of 100 g/ml and higher, and the death rate increased with each rise in concentration. While at greater concentrations of 200 and 400 g/ml, the normal cell was subjected to a lower death rate. The cytotoxic effect (IC50) of cells treated with Ag:Pectin NPs was increased up to 195 g/ml against skin cancer cells and a moderate rise of 250 g/ml for normal cells, it can be seen. At a greater concentration of 400 g/ml, the Ag:Pectin NPs had a higher death rate of roughly 34% for skin cancer cells and 20% for normal cells..

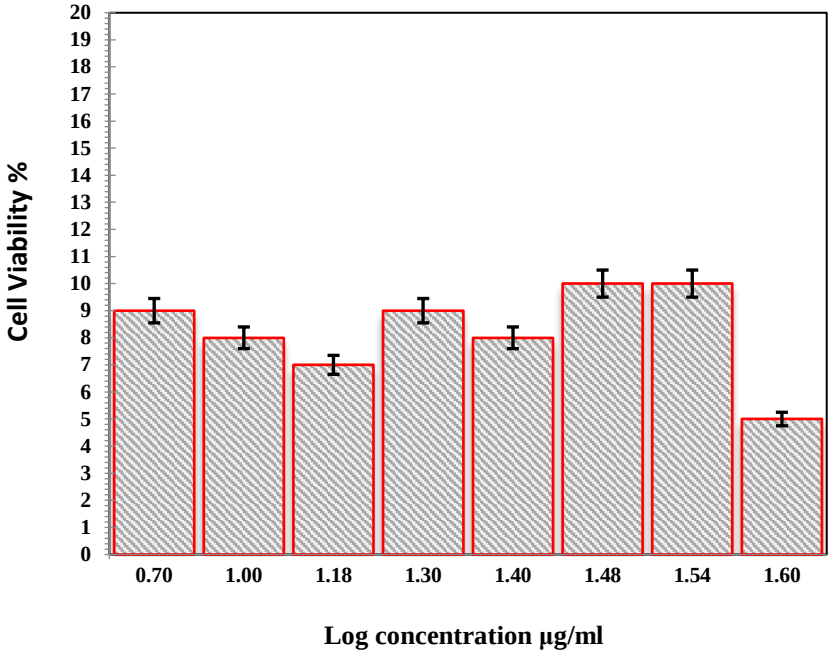

Figure -12 Cytoxicity analysis of Ag NPs by using laser method

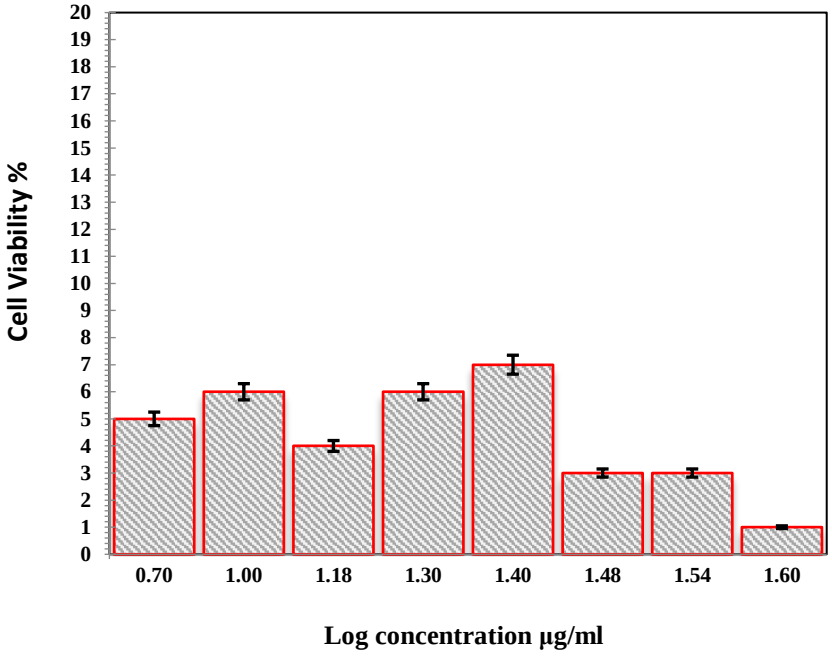

Figure -13 Cytotoxicity analysis of Ag: Pectin NPs by using laser method

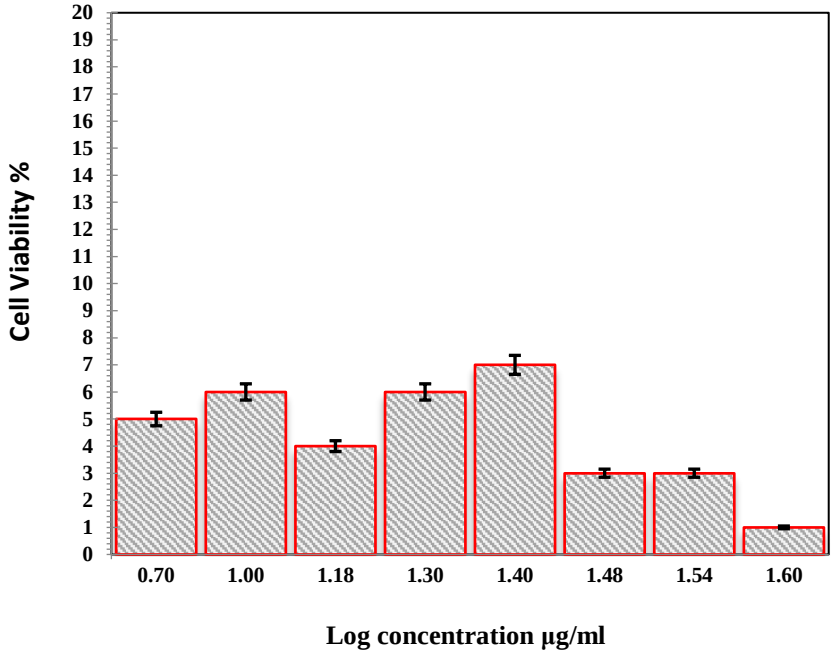

Figure -14 Cytotoxicity analysis of pectin by using laser method

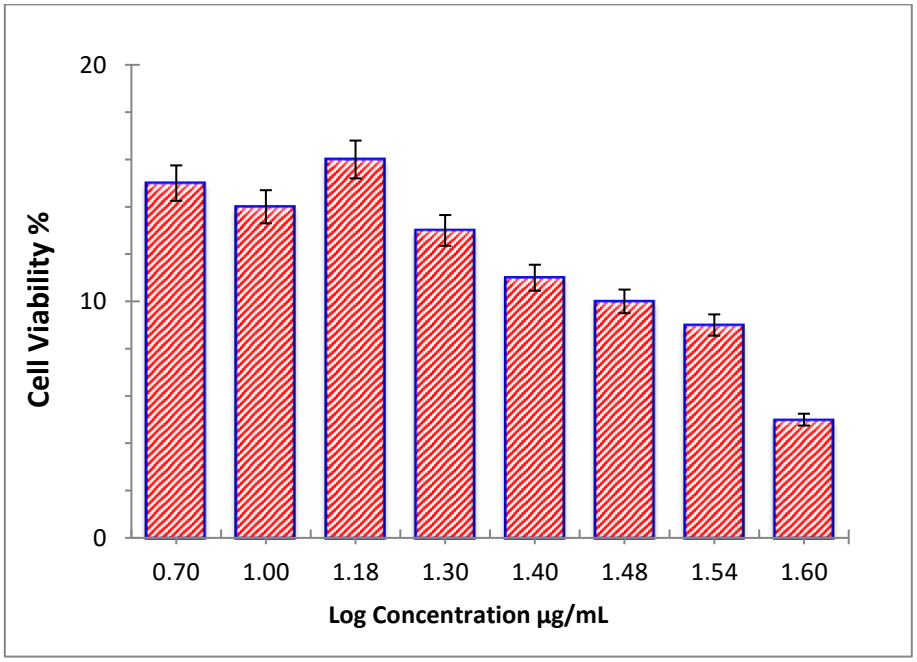

Figure -15 Cytotoxicity analysis of Ag NPs by using electrochemical method

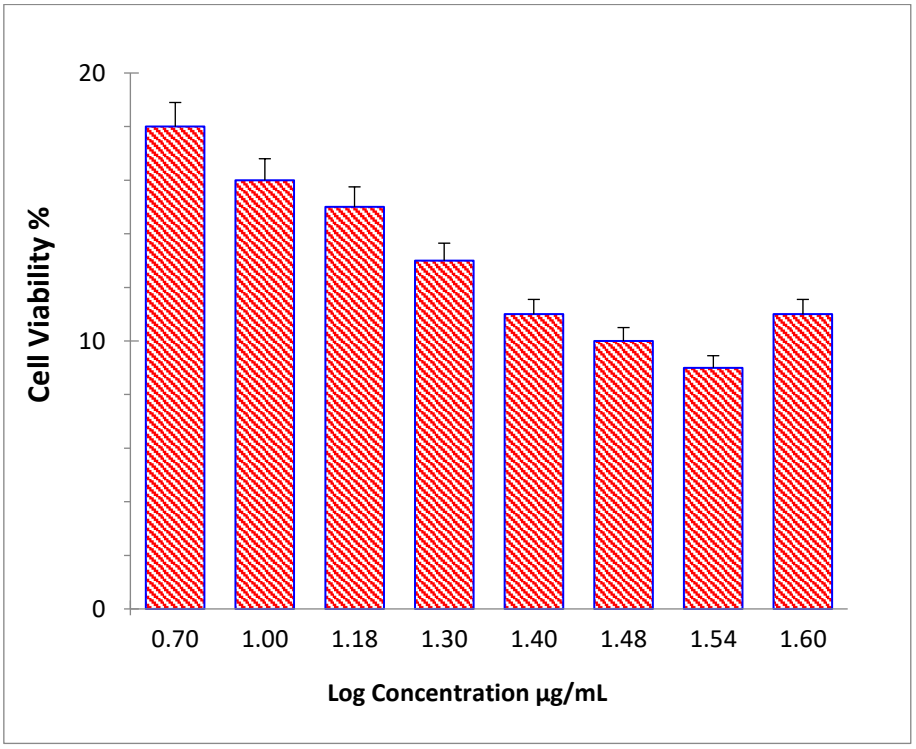

Figure -16 Cytotoxicity analysis of Ag: Pectin NPs by using electrochemical method

6. Antibacterial activity

In order to study the antibacterial activity of silver and silver: pectin nanoparticles against harmful organisms such Staphylococcus aureus, Salmonella typhi, Klebsiella pneumoniae, and Escherichia coli, various synthetic methods were used (Figure 17). The figure below shows the diameter of the inhibition zones (mm) surrounding each well with silver nanoparticle solution. Staphylococcus aureus (23 mm) and Salmonella typhi (21 mm) were the bacteria with the highest antibacterial activity (20 mm). The lesser antimicrobial activity was found against Escherichia coli (19 mm). Escherichia coli was shown to have decreased antibacterial action (19 mm). The Gram negative bacteria model E. coli was discovered to be susceptible to silver nanoparticles, demonstrating this substance's antimicrobial property[19] . Staphylococcus aureus and E. coli are both susceptible to the antibacterial effects of silver nanoparticles[20] . According to the results of the experiment, Gram positive Staphylococcus aureus was more susceptible to the nanoparticles than Gram negative Klebsiella pneumoniae, Salmonella typhi, and Escherichia coli. The clearest argument for Staphylococcus aureus' vulnerability to nanoparticles may be the organism's cell wall plasmolysis, or the detachment of its cytoplasm from its cell wall[21] . Depending on the size of the nanoparticles as well as the kind of bacteria, bio-nanosilver particles' antibacterial processes can vary.

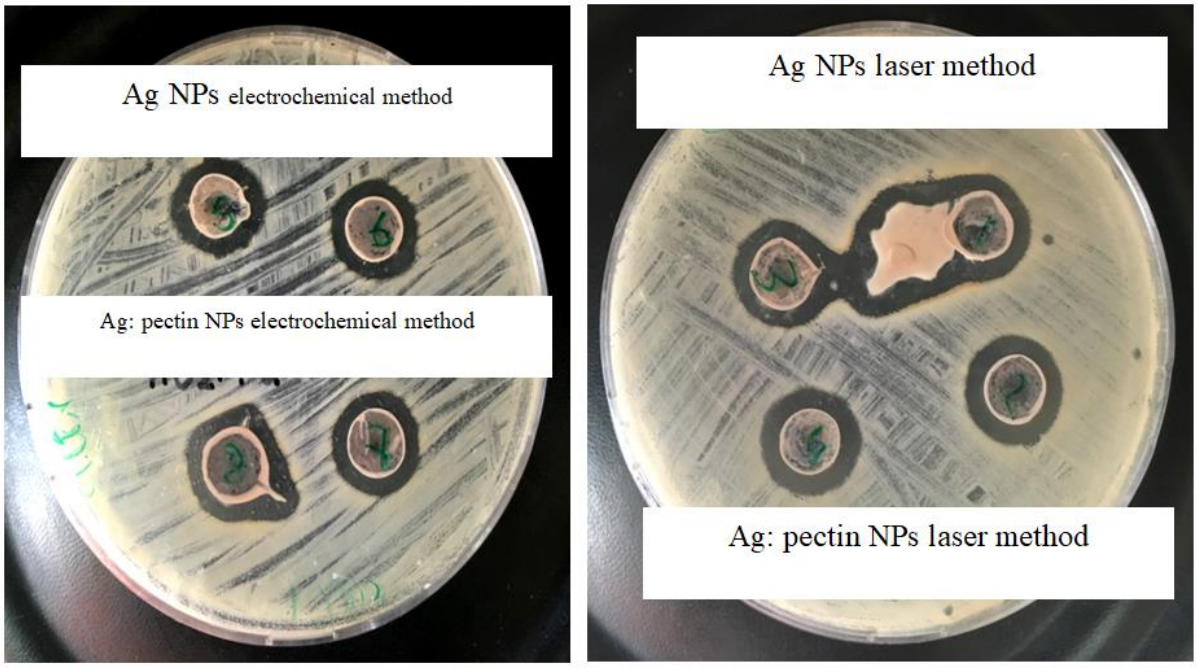

Figure -17 Antibacterial activities for both - preparation methods

The use of silver nanoparticle technology in cancer treatment has shown promising results. The features of silver nanoparticles, such as their small size, non-toxicity, shape and immunodeficiency, make them suitable candidates for targeted drug delivery systems. The ability to bypass the body's natural barriers becomes more plausible as tumor-targeted delivery routes decrease [13] . Tumor-specific ligands can be grafted onto particles using chemotherapy drug particles to allow these particles to circulate throughout the tumor without being redistributed in the body, increasing specificity and drug delivery potential [14] .The cell line screening method, the anti-tumor capacity, of Ag and Ag:pectin NPs were investigated in a colorectal cancer cell line. At varied doses (70-160 µg/ml), Ag and Ag:pectin NPs showed significant cytotoxicity against colorectal cancer cell line[9] . Ag and Ag:pectin NPs induced tumor cell death at a specific concentration of 160 µg/ml. With the increase in the amount of silver nanoparticles, the percentage of cell viability decreases in colorectal cancer cell line (Fig. 18) and (Fig. 19), this result agrees with[14] . A flow cytometer was used to examine the cellular uptake of Au nanosheets in a cancer cell line to better understand the factors that contribute to toxicity. The difference in incubation time was 0-120 min, Ag and Ag:pectin NPs were suspended in medium at two concentrations of 10 mM and 20 mM plus control cells and doses. Western blot technique was performed here to access the effects of Ag and Ag:pectin NPs from tumor cells as shown in the figure. (21) and (24) , protein levels decreased after treatments of Ag and Ag:pectin NPs.

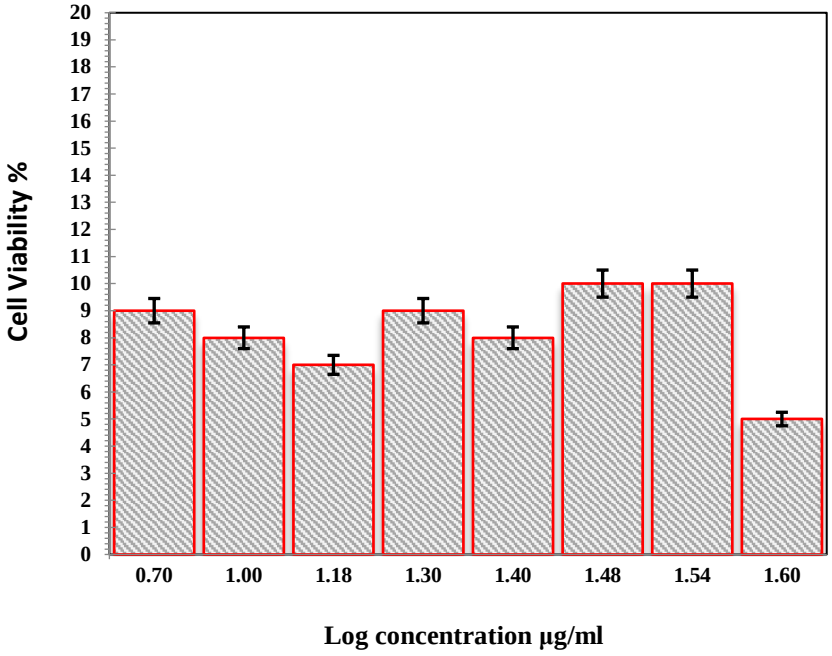

Figure -18 Cytotoxicity analysis of pectin by using laser method

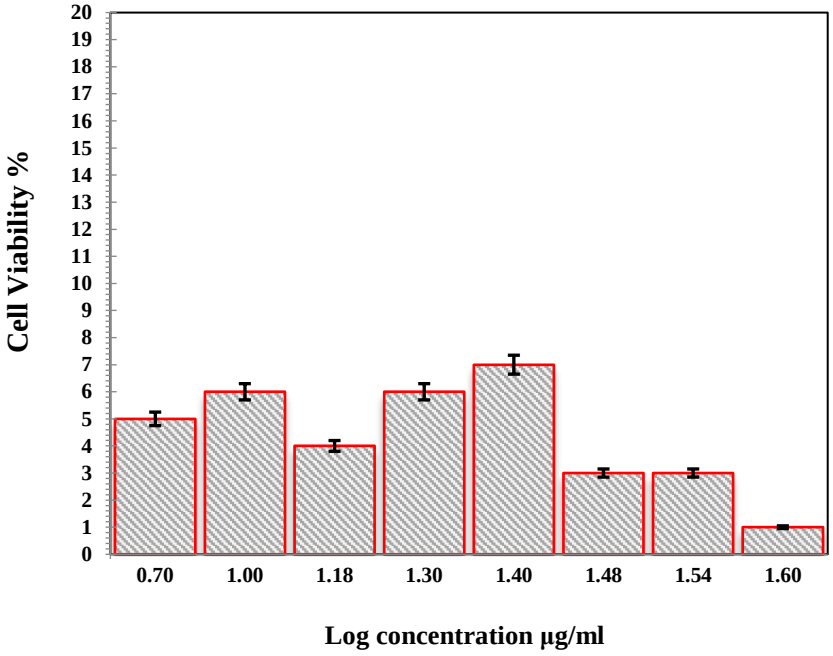

Ag NP

Figure -19 Cytotoxicity analysis of Ag@ Pectin NPs by using laser method

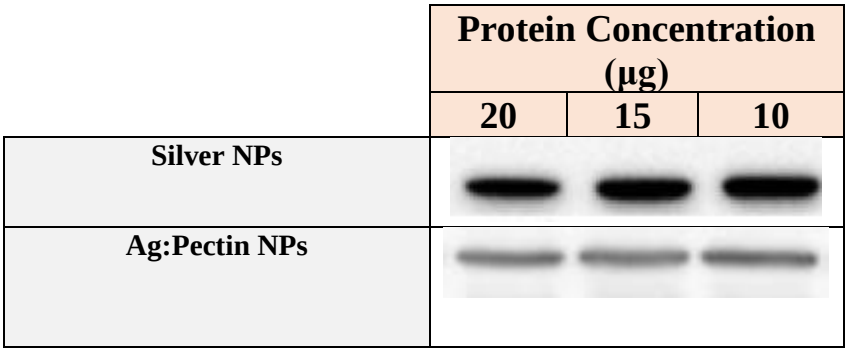

Figure -20 Westron blot analysis of Ag and Ag: Pectin NPs by using laser method

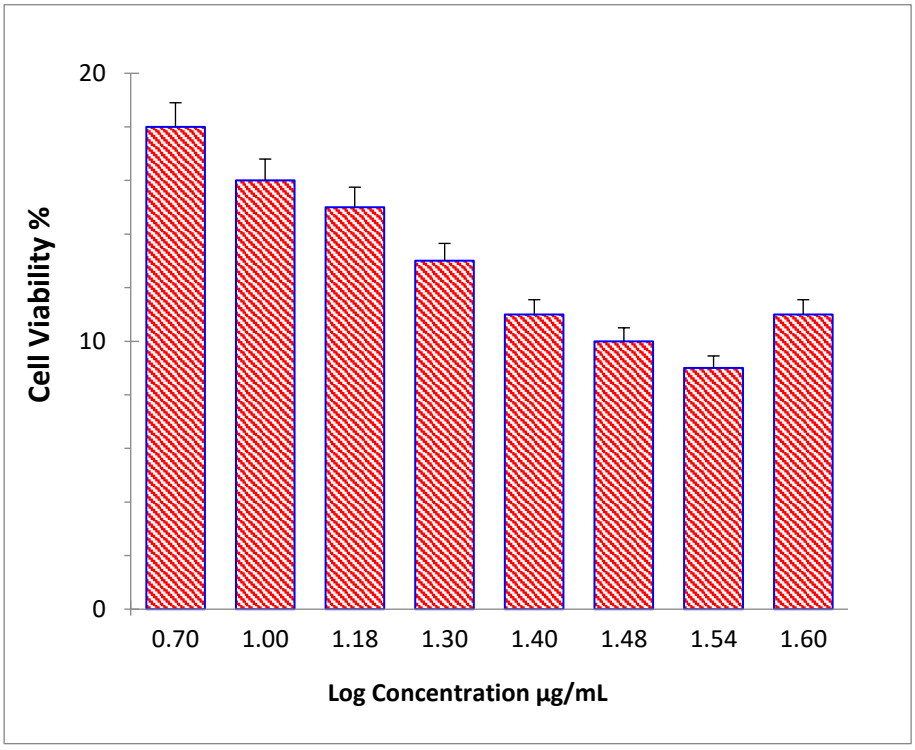

Figure -21 Cytotoxicity analysis of Ag@pectin NPs by using electrochemical method

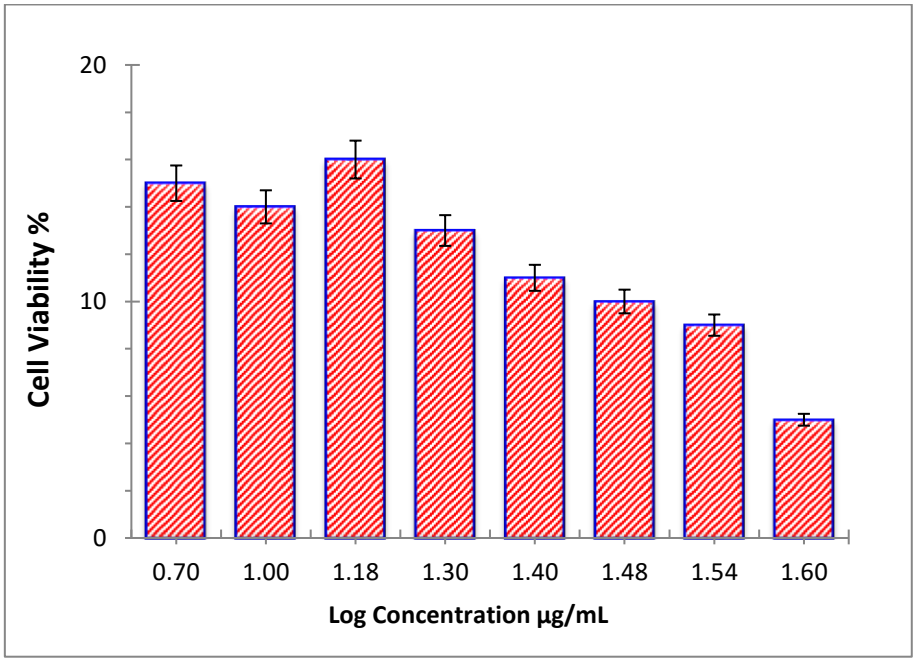

Figure -22 Cytotoxicity analysis of Ag NPs by using electrochemical method

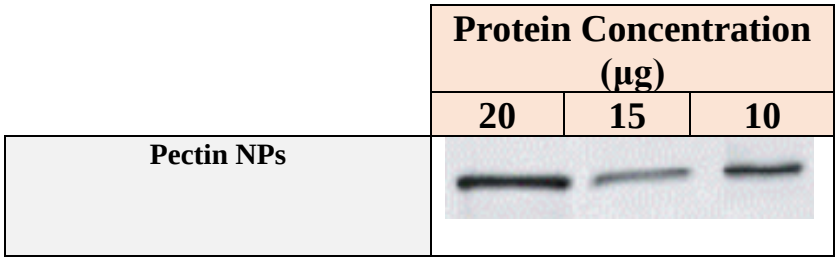

Figure -23 Westron blot analysis of Ag and Ag: Pectin NPs by using electrochemical method

7. Conclusions

The research on Ag:pectin NPs for their antibacterial activities and Pe-AuNPs for their anticancer and drug carrier activities both yielded positive results, according to the findings and discussion presented above. Our comprehensive analysis found that Ag:pectin NPs shown strong biological activity and were biocompatible and non-toxic, indicating that Ag and Au are acceptable metals that can be produced by pectin. The biological activities of Pe-MNPs, however, need additional study in the in vitro, in vivo, and clinical sectors to establish their efficacy due to the limitations of studies carried out throughout the years.

8. References

[1] S. E. Flores-Villaseñor, R. D. Peralta-Rodríguez, J. C. Ramirez-Contreras, G. Y. Cortes-Mazatán, and A. N. Estrada-Ramírez, "Biocompatible microemulsions for the nanoencapsulation of essential oils and nutraceuticals," in *Encapsulations*, Elsevier, 2016, pp. 503–558.

[2] D. Chen and N. K. Jha, "Introduction to nanotechnology," in *Nanoelectronic circuit design*, Springer, 2010, pp. 1–22.

[3] N. Sivagangi Reddy, K. Madhusudana Rao, T. J. Sudha Vani, K. S. V Krishna Rao, and Y. I. Lee, "Pectin/poly (acrylamide-co-acrylamidoglycolic acid) pH sensitive semi-IPN hydrogels: selective removal of Cu2+ and Ni2+, modeling, and kinetic studies," *Desalin. Water Treat.*, vol. 57, no. 14, pp. 6503–6514, 2016.

[4] J. F. Sargent, *The National Nanotechnology Initiative: overview, reauthorization, and appropriations issues*. Congressional Research Service, 2010.

[5] S. K. Nune, P. Gunda, P. K. Thallapally, Y.-Y. Lin, M. Laird Forrest, and C. J. Berkland, "Nanoparticles for biomedical imaging," *Expert Opin. Drug Deliv.*, vol. 6, no. 11, pp. 1175–1194, 2009.

[6] G. Wang, "Nanotechnology: The new features," *arXiv Prepr. arXiv1812.04939*, 2018.

[7] P. Kumar *et al.*, "Comprehensive survey on nanobiomaterials for bone tissue engineering applications," *Nanomaterials*, vol. 10, no. 10, p. 2019, 2020.

[8] E. C. Njagi *et al.*, "Biosynthesis of iron and silver nanoparticles at room temperature using aqueous sorghum bran extracts," *Langmuir*, vol. 27, no. 1, pp. 264–271, 2011.

[9] P. Mohanpuria, N. K. Rana, and S. K. Yadav, "Biosynthesis of nanoparticles: technological concepts and future applications," *J. nanoparticle Res.*, vol. 10, pp. 507–517, 2008.

[10] M. Sastry, A. Ahmad, M. I. Khan, and R. Kumar, "Biosynthesis of metal nanoparticles using fungi and actinomycete," *Curr. Sci.*, pp. 162–170, 2003.

[11] W. G. T. Willats, L. McCartney, W. Mackie, and J. P. Knox, "Pectin: cell biology and prospects for functional analysis," *Plant Mol. Biol.*, vol. 47, pp. 9–27, 2001.

[12] J.-P. Vincken *et al.*, "If homogalacturonan were a side chain of rhamnogalacturonan I. Implications for cell wall architecture," *Plant Physiol.*, vol. 132, no. 4, pp. 1781–1789, 2003.

[13] H. Kokkonen, C. Cassinelli, R. Verhoef, M. Morra, H. A. Schols, and J. Tuukkanen, "Differentiation of osteoblasts on pectin-coated titanium," *Biomacromolecules*, vol. 9, no. 9, pp. 2369–2376, 2008.

[14] H. Towbin, "Electrophoretic transfer of proteins from polyacrylamide gels to nitrocellulose sheets: procedure and some applications. 1979 [classical article]," *Biotechnology*, vol. 24, pp. 145–149, 1992.

[15] L. S. Dorobantu and M. R. Gray, "Application of atomic force microscopy in bacterial research," *Scanning*, vol. 32, no. 2, pp. 74–96, 2010.

[16] S. H. Jumaah, M. R. Hussein, N. F. Habubi, S. S. Chiad, and K. H. Abass, "Improving the Antibacterial Properties of SnO 2/Mn 3 O 4 Hybrid Thin Film Synthesized by Spray Pyrolysis Method.," *Nano Biomed. Eng.*, vol. 14, no. 3, 2022.

[17] L. Karthik, G. Kumar, A. V. Kirthi, A. A. Rahuman, and K. V Bhaskara Rao, "Streptomyces sp. LK3 mediated synthesis of silver nanoparticles and its biomedical application," *Bioprocess*

Biosyst. Eng., vol. 37, pp. 261–267, 2014.

[18] J. Dolinska *et al.*, "Noble metal nanoparticles in pectin matrix. Preparation, film formation, property analysis, and application in electrocatalysis," *ACS omega*, vol. 5, no. 37, pp. 23909–23918, 2020.

[19] S. B. Brown, E. A. Brown, and I. Walker, "The present and future role of photodynamic therapy in cancer treatment," *Lancet Oncol.*, vol. 5, no. 8, pp. 497–508, 2004.

[20] M. Wainwright, "Photodynamic antimicrobial chemotherapy (PACT).," *J. Antimicrob. Chemother.*, vol. 42, no. 1, pp. 13–28, 1998.

[21] P. K. Sake, B. Rajeswari, V. Reddy, P. S. Khan, and G. Damu, "Isolation and quantification of flavonoid from euphorbia antiquorum latex and its antibacterial studies," *Indian J. Adv. Chem. Sci. 1 117*, vol. 122, 2013.